THE ASTROPHYSICAL JOURNAL, 250:739–749, 1981 November 15

ON THE EVOLUTION OF THE HOMOGENEOUS ELLIPSOIDAL FIGURES. II. GRAVITATIONAL COLLAPSE AND GRAVITATIONAL RADIATION

STEVEN DETWEILER
Department of Physics, Yale University

AND

LEE LINDBLOM
Department of Physics, University of California, Santa Barbara, and Department of Physics, Stanford University
Received 1981 March 23; accepted 1981 May 19

ABSTRACT

We use homogeneous ellipsoids to model the gravitational collapse of a stellar core and the subsequent emission of gravitational radiation. The growth of asymmetry caused by the collapse is computed along with the flux and energy spectrum of the gravitational radiation produced as the ellipsoid evolves toward an axisymmetric state following the collapse. In the very low angular momentum limit we find that a 1 $M_\odot$ core of radius $R=10^6$ cm and angular velocity $\Omega_p=10^3$ s^{-1} should emit gravitational radiation by this mechanism with a total energy of approximately $E_{GR}=10^{-6}\ Mc^2$, at a frequency of 1600 Hz and a bandwidth of only about 1.6 Hz.

Subject headings: gravitation — radiation mechanisms — stars: collapsed — stars: interiors

I. INTRODUCTION

In this paper we extend the analysis of the slowly evolving ellipsoidal figures by Detweiler and Lindblom (1977, hereafter referred to as Paper I) to model the gravitational collapse of a stellar core and the subsequent emission of gravitational radiation. We limit our attention here to only one class of nonaxisymmetric ellipsoids: those whose angular velocities and vorticities are parallel to one of the principal axes of the ellipsoid. In the stationary case these are the Riemann S ellipsoids (see, e.g., Chandrasekhar 1969, hereafter referred to as E.F.E.). This special case enables us to study the collapse and subsequent emission of gravitational radiation in a thorough, comprehensive manner. Also this particular type of asymmetry is amplified by secular instabilities in sufficiently rapidly rotating ellipsoids. Any energy in the ellipsoid associated with the other types of asymmetric motions is also radiated away before the model settles down to an axisymmetric Maclaurin spheroid. Therefore, our estimates of the energies and fluxes of gravitational radiation could be considered lower limits.

Our treatment of the gravitational collapse of the stellar core is formally equivalent to Lebovitz's (1972, 1974) method of studying the collapse of a protostellar gas cloud. We compute the growth of the asymmetry in a collapsing ellipsoid by assuming that the angular momentum and circulation of the ellipsoid are conserved during the collapse. This assumption is valid whenever the viscous and gravitational radiation dissipation time scales are longer than the collapse time scale, and it allows us to compute the final asymmetry of the ellipsoid as a function of its initial asymmetry and the ratio, ρ/ρ_0, of the final and initial densities of the ellipsoid.

This treatment of the gravitational collapse of the ellipsoidal model is simplistic and does not determine how the gravitational potential energy is released during the collapse. We concentrate instead on determining how the nonaxisymmetry of the ellipsoid is radiated away by gravitational radiation. Under the assumption that this process occurs much more slowly than the collapse itself, the equilibrium ellipsoidal model of neutron star density begins with an asymmetry determined by our collapse calculations. We then compute the luminosity and spectrum of gravitational radiation emitted by such a model as it evolves toward an axisymmetric Maclaurin spheroid. The luminosity and total energy radiated by this mechanism are smaller than that produced during the initial dynamic collapse of the ellipsoid (Saenz and Shapiro 1978, 1979, 1980), but the spectrum is very narrow banded. The resulting high spectral densities may be more easily observed by certain types of gravitational wave detectors.

We perform the analysis of the collapse and subsequent emission of gravitational radiation described above in two different ways in the following sections. In § II we derive the general equations which describe these processes in the ellipsoidal figures having angular velocities and vorticities parallel to one of the principle axes of the ellipsoid. These equations are solved numerically, and the results are displayed graphically for an essentially complete sampling of ellipsoidal figures (having angular velocities exceeding their vorticity parameters $|\Omega|>|\Lambda|$).

In § III we concentrate on the physically most interesting case: nearly axisymmetric ellipsoids. For this special case the equations simplify sufficiently that analytic solutions are obtained for the various quantities of interest. In § IV we consider the astrophysical significance of these computations by estimating the luminosities, frequencies, and bandwidths of gravitational radiation for models having realistic neutron star parameters.

II. GENERAL ELLIPSOIDS

a) Equations of Motion

We review here the equations of motion for an ellipsoidal figure whose angular velocity and vorticity axes are parallel to one of the principal axes of the ellipsoid. These equations have been given in general in Paper I and E.F.E. We consider an ellipsoid having principal axes of lengths a_1, a_2, and a_3, a mass density ρ (which is uniform but may be time dependent), total mass M, angular velocity Ω about the a_3 axis, and a uniform vorticity in the a_3 direction parametrized by Λ. The equations of motion for such an ellipsoid are simple if the ellipsoid collapses much faster than the viscous time scales and if the evolution at uniform density due to gravitational radiation reaction takes much longer than a typical hydrodynamical oscillation of the ellipsoid. Under these conditions the angular velocity Ω and the vorticity parameter Λ are considered as functions of the a_i and the density ρ given by

$$(\Lambda \pm \Omega)^2 = 2\pi G\rho\left[\frac{a_1A_1 \mp a_2A_2}{a_1 \mp a_2} \pm \frac{a_3{}^2A_3}{a_1a_2}\right], \tag{1}$$

where the index symbols A_i are functions of the a_i defined by the integrals:

$$A_i = \int_0^\infty a_1a_2a_3(a_i^2+u)^{-1}\left[(a_1{}^2+u)(a_2{}^2+u)(a_3{}^2+u)\right]^{-1/2} du. \tag{2}$$

The evolution of these ellipsoids is governed by the equations

$$\begin{pmatrix} a_1 & -a_2 \\ -a_2 & a_1 \end{pmatrix}\begin{pmatrix} \dot{\Lambda} \\ \dot{\Omega} \end{pmatrix} + 2\begin{pmatrix} \Lambda & -\Omega \\ \Omega & -\Lambda \end{pmatrix}\begin{pmatrix} \dot{a}_1 \\ \dot{a}_2 \end{pmatrix} = -16\mathcal{G}\Omega^5(a_1{}^2-a_2{}^2)\begin{pmatrix} a_2 \\ a_1 \end{pmatrix}, \tag{3}$$

and by the conservation of mass

$$\dot{a}_1/a_1 + \dot{a}_2/a_2 + \dot{a}_3/a_3 = -\dot{\rho}/\rho, \tag{4}$$

where a dot signifies d/dt, $\mathcal{G} = 2GM/25c^5$, G is the gravitational constant, and c is the speed of light.

Equations (3) and (4) determine the time development of the lengths of the principal axes of the ellipsoid, a_i, while equation (1) in turn determines Λ and Ω.

These equations can be cast into an equivalent form which is often useful. The total mass of the ellipsoid M, the total angular momentum L, the circulation of the fluid about an equatorial contour at the surface of the ellipsoid C, and the total kinetic and gravitational energy of the ellipsoid E are related to the parameters of the ellipsoid introduced earlier by the equations:

$$M = \tfrac{4}{3}\pi a_1a_2a_3\rho, \tag{5}$$

$$L = \tfrac{1}{5}M\left[(a_1{}^2+a_2{}^2)\Omega - 2a_1a_2\Lambda\right], \tag{6}$$

$$C = \pi\left[2a_1a_2\Omega - (a_1{}^2+a_2{}^2)\Lambda\right], \tag{7}$$

$$E = \tfrac{1}{5}M\left[\tfrac{1}{2}(a_1{}^2+a_2{}^2)(\Lambda^2+\Omega^2) - 2a_1a_2\Omega\Lambda - 2\pi G\rho\sum_i a_i^2A_i\right]. \tag{8}$$

It follows from equations (1)–(4) that the time development of these quantities are given by

$$dM/dt = dC/dt = 0, \tag{9}$$

$$dL/dt = -\tfrac{16}{5} M \mathcal{G} \Omega^5 (a_1{}^2 - a_2{}^2)^2, \tag{10a}$$

and when $\dot{\rho} = 0$,

$$dE/dt = \Omega\, dL/dt. \tag{10b}$$

Thus the mass and circulation are conserved quantities as the ellipsoid evolves, while the angular momentum and energy decrease as gravitational radiation is emitted.

b) Collapse

We model the gravitational collapse of a stellar core by computing a family of equilibrium ellipsoids, each having the same total mass, angular momentum, and equatorial circulation as the precollapse ellipsoidal model. This is appropriate whenever the collapse and the associated radiation of the gravitational potential energy (primarily by the neutrinos) occur on a time scale which is shorter than the time scale associated with the dissipation of angular momentum by gravitational radiation and the dissipation of circulation by neutrino viscosity. This situation is expected to be the case for postcollapse stellar cores with densities up to about 10^{13} g cm^{-3} (see Lindblom and Detweiler 1979).

We consider a family of equilibrium ellipsoids parametrized by their density $a_i(\rho)$, $\Lambda(\rho)$, $\Omega(\rho)$ which have the same angular momentum, equatorial circulation, and mass; consequently,

$$dM/d\rho = dC/d\rho = dL/d\rho = 0. \tag{11}$$

The requirement that each member of the family be an equilibrium model which satisfies equation (1), completely determines the family of ellipsoids. These equations are equivalent to equations (1)–(4) where the gravitational radiation parameter $\mathcal{G}$ has been set to zero, and the time parameter has been replaced by ρ.

To convert equation (11) to a form which gives information about the way the shape of the ellipsoid evolves as the density changes, we replace the parameters a_i by R, the average radius of the ellipsoid, and two asymmetry parameters, α_2, and α_3, defined by $R^3 = a_1 a_2 a_3$, $\alpha_2 = a_2/a_1$, and $\alpha_3 = a_3/a_1$. The axes of the ellipsoid are labeled so that $\alpha_i < 1$. The mass is constant for each family of ellipsoids, so the change in R as the density changes is easily computed from equation (5):

$$R = \left(\frac{3M}{4\pi\rho}\right)^{1/3}. \tag{12}$$

The asymmetry parameters α_2 and α_3 are determined from the conservation of C and L. While these first integrals of equation (11) are known, they are in practice extremely difficult to "invert" to determine the final values of α_2 and α_3. We find it easier to simply integrate equation (11) numerically. Now we describe in detail how this is done. Note that the index symbols A_i are functions only of α_2 and α_3 and do not depend on R (as can be easily verified from eq. [2]). Therefore, the quantities $\Omega^* \equiv \Omega/(2\pi G\rho)^{1/2}$ and $\Lambda^* \equiv \Lambda/(2\pi G\rho)^{1/2}$ are functions only of α_2 and α_3 which can be explicitly computed (by numerically evaluating the integrals A_i) from equation (2). Similarly, the functions $\partial\Omega^*/\partial\alpha_2, \partial\Lambda^*/\partial\alpha_2$, etc., can be explicitly computed (by numerically evaluating the integrals A_i and $\partial A_i/\partial\alpha_2$, etc.). Thus the derivatives of Ω^* and Λ^* with respect to ρ can be related to the derivatives of α_2, α_3:

$$\begin{pmatrix} \dfrac{d\Omega^*}{d\rho} \\ \dfrac{d\Lambda^*}{d\rho} \end{pmatrix} = \begin{pmatrix} \dfrac{\partial\Omega^*}{\partial\alpha_2} & \dfrac{\partial\Omega^*}{\partial\alpha_3} \\ \dfrac{\partial\Lambda^*}{\partial\alpha_2} & \dfrac{\partial\Lambda^*}{\partial\alpha_3} \end{pmatrix} \begin{pmatrix} \dfrac{d\alpha_2}{d\rho} \\ \dfrac{d\alpha_3}{d\rho} \end{pmatrix}. \tag{13}$$

Another expression for the derivatives of Ω^* and Λ^* can be obtained by explicitly writing out equations (11) using the definitions of C and L from equations (6) and (7). The resulting equations have the following form:

$$\begin{pmatrix} \dfrac{d\Omega^*}{d\rho} \\ \dfrac{d\Lambda^*}{d\rho} \end{pmatrix} = \begin{pmatrix} B_{12} & B_{13} \\ B_{22} & B_{23} \end{pmatrix} \begin{pmatrix} \dfrac{d\alpha_2}{d\rho} \\ \dfrac{d\alpha_3}{d\rho} \end{pmatrix} + \frac{1}{\rho} \begin{pmatrix} B_1 \\ B_2 \end{pmatrix}, \tag{14}$$

where the B_i and the B_{ij} are explicit functions of α_2 and α_3 given by:

$$B_{12} = \tfrac{2}{3}\left[3\Lambda^* + \left(2\alpha_2 + \alpha_2^{-1}\right)\Omega^*\right]/\left(1-\alpha_2^2\right), \tag{15}$$

$$B_{13} = \tfrac{2}{3}\Omega^*/\alpha_3, \tag{16}$$

$$B_{22} = \tfrac{2}{3}\left[3\Omega^* + \left(2\alpha_2 + \alpha_2^{-1}\right)\Lambda^*\right]/\left(1-\alpha_2^2\right), \tag{17}$$

$$B_{23} = \tfrac{2}{3}\Lambda^*/\alpha_3, \tag{18}$$

$$B_1 = \tfrac{1}{6}\Omega^*, \tag{19}$$

$$B_2 = \tfrac{1}{6}\Lambda^*. \tag{20}$$

Therefore, combining equations (13) and (14), we obtain a system of first order differential equations for $\alpha_2(\rho)$ and $\alpha_3(\rho)$:

$$\begin{pmatrix} B_{12} - \partial\Omega^*/\partial\alpha_2 & B_{13} - \partial\Omega^*/\partial\alpha_3 \\ B_{22} - \partial\Lambda^*/\partial\alpha_2 & B_{23} - \partial\Lambda^*/\partial\alpha_3 \end{pmatrix} \begin{pmatrix} d\alpha_2/d\rho \\ d\alpha_3/d\rho \end{pmatrix} + \rho^{-1} \begin{pmatrix} B_1 \\ B_2 \end{pmatrix} = 0. \tag{21}$$

Equations (21) have been integrated numerically and the results are presented in Figures 1 and 2. The curves plotted in these figures represent families of ellipsoids having the same mass, angular momentum, and circulation. The parameter along these curves is $\log_{10} \rho$ and is indicated in the figures by the series of black dots. The difference in parameter between dots is 0.5; therefore, the density increases by a factor of 10 every two dots along these curves. Note that as a consequence of equation (21) the curves do not depend on the absolute value of the density, so these curves are generally applicable to a wide range of collapse problems from protostellar formation to the final collapse of a

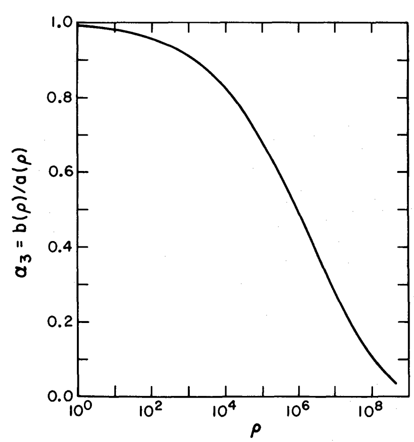

FIG. 1

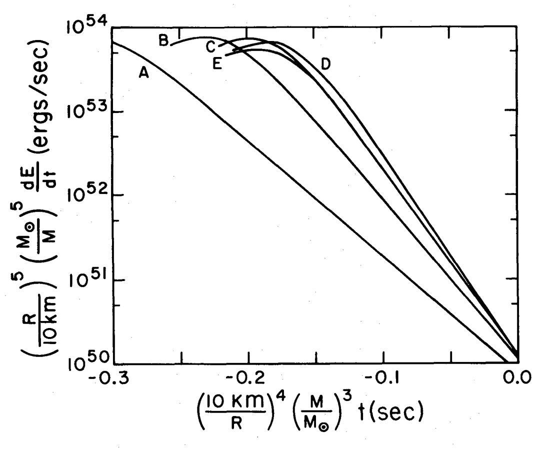

FIG. 2

FIG. 1.—The change of the two asymmetry parameters $\alpha_2(\rho)$ and $\alpha_3(\rho)$ is depicted as the density of an ellipsoid is varied. Every two dots along the curve represent a factor of 10 in the density.

FIG. 2.—A magnified view of the nearly axisymmetric portion of Fig. 1.

stellar core to form a neutron star. The general direction of evolution along these curves as the density of the ellipsoid increases is from the upper right toward the lower left. Thus the asymmetry of the ellipsoid grows as it collapses. Also note that each curve tends to become parallel to the lower self-adjoint sequence of Riemann S ellipsoids, whereupon the asymmetry grows very quickly as the density increases. Lebovitz (1972, 1974) has argued that this will lead to fragmentation (see also Boss 1980). It is also clear that if an ellipsoid can collapse to this highly asymmetric configuration, large amounts of gravitational radiation will be emitted.

c) *Gravitational Radiation*

When the density is taken to be constant in § II*a*, the same equations describe the evolution of an ellipsoid under the influence of gravitational radiation. These equations can be reduced to a system of equations which represent the time development of α_2 and α_3 in much the same way as the collapse of the ellipsoid was described in § II*b*. Thus

$$\begin{pmatrix} d\Omega^*/dt \\ d\Lambda^*/dt \end{pmatrix} = \begin{pmatrix} B_{12} & B_{13} \\ B_{22} & B_{23} \end{pmatrix} \begin{pmatrix} d\alpha_2/dt \\ d\alpha_3/dt \end{pmatrix} + \begin{pmatrix} B_1' \\ B_2' \end{pmatrix}, \tag{22}$$

where the B_{ij} are given by eqs. (15)–(18) and B_1' and B_2' are defined by:

$$B_1' = -64\pi^2 G^2 \rho^2 \mathcal{G} R^2 \Omega^{*5}(1+\alpha_2^2)/(\alpha_2\alpha_3)^{2/3}, \tag{23}$$

$$B_2' = -128\pi^2 G^2 \rho^2 \mathcal{G} R^2 \Omega^{*5} \alpha_2/(\alpha_2\alpha_3)^{2/3}. \tag{24}$$

Furthermore, with equation (13), the final equations for the evolution of α_2 and α_3 are given by

$$\begin{pmatrix} B_{12} - \partial\Omega^*/\partial\alpha_2 & B_{13} - \partial\Omega^*/\partial\alpha_3 \\ B_{22} - \partial\Lambda^*/\partial\alpha_2 & B_{23} - \partial\Lambda^*/\partial\alpha_3 \end{pmatrix} \begin{pmatrix} d\alpha_2/dt \\ d\alpha_3/dt \end{pmatrix} + \begin{pmatrix} B_1' \\ B_2' \end{pmatrix} = 0. \tag{25}$$

These equations can be solved numerically in a straightforward fashion for the time evolution of α_2 and α_3. Figure 3 represents these paths for several possible choices of initial conditions. Note that equation (25) implies that these paths are independent of the total mass, mass density, and radius of the ellipsoid. These parameters only determine the rate at which the ellipsoid evolves along the path. The parametrization shown in Figure 3 is that for a 1 $M_\odot$ model with average radius 10^6 cm. The time $t=0$ is arbitrarily set when $\alpha_2 = 0.99$ and adjacent points on the curves differ by 0.05 s. For models with other values of M and R, this time interval between tick marks on the curves should be

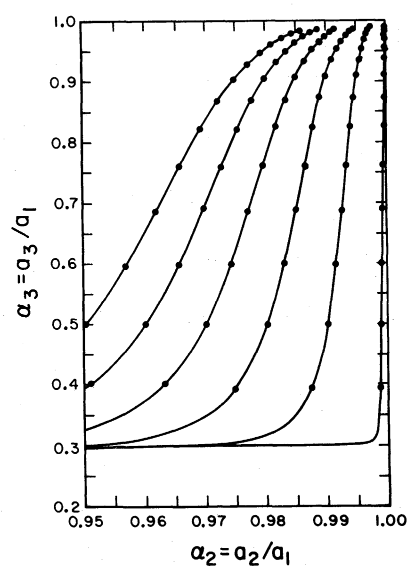

FIG. 3.—The evolutionary tracks $\alpha_2(t)$, $\alpha_3(t)$ of several ellipsoidal models evolving by the emission of gravitational radiation. Adjacent dots differ in time by 0.05 s. Various properties of the gravitational radiation which is emitted by these models are depicted in Figs. 4–6.

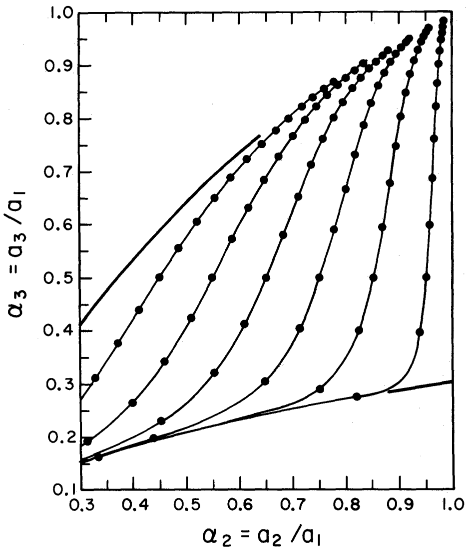

FIG. 4

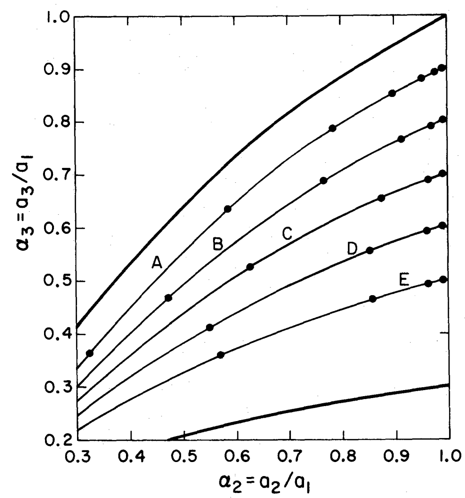

FIG. 5

FIG. 4.—The gravitational wave luminosity as a function of time for the ellipsoidal models depicted in Fig. 3.
FIG. 5.—The frequency of the gravitational radiation emitted as a function of time for the ellipsoidal models depicted in Fig. 3.

multiplied by the factor

$$(M/M_{\odot})^{-3}(R/10^6\ \mathrm{cm})^4.$$

As the ellipsoid evolves in the models, it emits gravitational radiation with frequency $\nu = \Omega/\pi$ and luminosity given by equation (10). Since the values of $\alpha_2(t)$ and $\alpha_3(t)$ are determined numerically, it is straightforward to determine $\Omega(t)$ and even $d\Omega/dt$ by evaluating equations (1) and (22). Thus we determine numerically the time evolution of the luminosity of gravitational radiation and the evolution of the frequency of this radiation for the evolutionary models depicted in Figure 3. The luminosity is depicted in Figure 4 while the frequency is given in Figure 5.

For the models presented in Figure 3 we have also computed the energy spectrum of gravitational radiation. This quantity is simply computed (as a function of time) from our evolutionary models by using

$$dE/d\nu = \pi(dE/dt)/(d\Omega/dt). \qquad (26)$$

This function is converted to a function of frequency by using the inverse of the function $\nu(t)$ given in Figure 5. The resulting energy spectrum $dE/d\nu$ is illustrated in Figure 6. This measure of the energy emitted in each frequency interval is approximately equivalent to the spectral density (defined in terms of the Fourier transform of the waveform) in the limit of slow evolution. Our measure is much easier to compute.

The typical luminosity produced by one of our models is smaller than that computed by Saenz and Shapiro (1978, 1979, 1980) for the initial dynamical stage of the collapse. But the energy emitted per frequency interval is considerably larger, which may make this radiation more easily detectable by certain types of gravitational radiation detectors.

III. NEARLY AXISYMMETRIC ELLIPSOIDS

a) Notation

In this section we establish the notation which will be used to describe a nearly axisymmetric slowly evolving ellipsoid model of the type considered in § II*a*. We assume that the principal axes of these models can be expressed in the form: $a_1 = a + \delta a_1$, $a_2 = a + \delta a_2$, and $a_3 = b + \delta a_3$, where a and b are the given parameters of the Maclaurin spheroid to which the model is to be compared and the δa_i are small and possibly time-dependent functions. We consider the equations of motion for these ellipsoids accurate through first order in the δa_i.

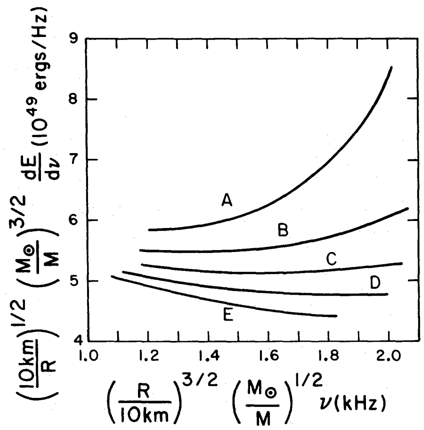

FIG. 6.—A measure of the energy of gravitational radiation emitted in each frequency interval for the ellipsoidal models depicted in Fig. 3.

The number of independent functions in this problem is reduced (as in the case for the general ellipsoids) by using the conservation of mass equation (4) and the equation for Λ and Ω, equation (1). The function δa_3 is expressed in terms of δa_1 and δa_2, from equation (4):

$$\delta a_3 = -(b/a)(\delta a_1 + \delta a_2). \tag{27}$$

The expressions for Λ and Ω, correct through first order, are obtained from an expansion of the right-hand side of equation (1). The resulting expressions have the form:

$$\Lambda = \Lambda_0 + \Lambda_1(\delta a_1 + \delta a_2), \tag{28}$$

$$\Omega = \Omega_0 + \Omega_1(\delta a_1 + \delta a_2), \tag{29}$$

where the Λ_0, Ω_0, Λ_1, and Ω_1 are certain explicit functions of a and b, given by:

$$(\Lambda_0 - \Omega_0)^2 = 2\pi G\rho[A_1 - 2(b/a)^2(1-A_1)], \tag{30}$$

$$(\Lambda_0 + \Omega_0)^2 = 2\pi G\rho[A_1 + 2(b/a)^2(1-A_1) + a(A_{11} - A_{12})], \tag{31}$$

$$\Lambda_1 - \Omega_1 = \frac{\pi G\rho}{\Lambda_0 - \Omega_0}\left\{6b^2a^{-3}(1-A_1) + \frac{1}{2}(1+2b^2a^{-2})[A_{11} + A_{12} - 2(b/a)A_{13}]\right\}, \tag{32}$$

$$\Lambda_1 + \Omega_1 = \frac{\pi G\rho}{\Lambda_0 - \Omega_0}\left[-\frac{6b^2}{a^3}(1-A_1) + A_{11} - \frac{b}{a}A_{13} + \frac{b^2}{a^2}\left(A_{31} - \frac{b}{a}A_{33}\right) + \frac{1}{2}a\left(A_{111} - A_{122} + \frac{b}{a}A_{123} - \frac{b}{a}A_{113}\right)\right]. \tag{33}$$

The symbols A_{ij} used in equations (30)–(33) are defined by $A_{ij} = \partial A_i/\partial a_j$ while the A_{ijk} are defined by $A_{ijk} = \partial^2 A_i/\partial a_j \partial a_k$.

In the limit of spherical symmetry, $a = b$, the equations derived above have a particularly simple form. Then equation (1) becomes:

$$(\Lambda - \Omega)^2 = 2\pi G\rho[\tfrac{4}{5}a^{-1}(\delta a_1 + \delta a_2)], \tag{34}$$

$$(\Lambda + \Omega)^2 = 2\pi G\rho[\tfrac{8}{15} - \tfrac{48}{35}a^{-1}(\delta a_1 + \delta a_2)]. \tag{35}$$

b) *Collapse*

The gravitational collapse of a nearly axisymmetric ellipsoid results in another nearly axisymmetric ellipsoid, as long as the density increase is not too large. This feature is manifest in the numerical integrations of the collapse problem depicted in Figures 1 and 2. In this section, therefore, we consider a sequence of nearly axisymmetric ellipsoids $a_1(\rho)=a(\rho)+\delta a_1(\rho), \Omega(\rho)=\Omega_0(\rho)+\Omega_1[\delta a_1(\rho)+\delta a_2(\rho)]$, etc., each of which has the same total mass, angular momentum, and circulation. The lowest order term of the mass conservation equation determines the average radius, $R^3=a^2b$, as a function of ρ according to eq. (12). Similarly the dependence of $\alpha_3=b/a$ on ρ follows from eq. (21) by setting $\alpha_2=1$. The resulting equation has the following simple form:

$$d\left[\rho^{-1/6}\alpha_3^{-2/3}(\Lambda_0{}^*-\Omega_0{}^*)\right]/d\rho=0. \tag{36}$$

This equation has been integrated numerically to determine $\alpha_3(\rho)$, and the result is depicted in Figure 7. The density units used in this figure are arbitrary and can be multiplied by any constant to make the graph applicable to any axisymmetric collapse problem in the ellipsoidal approximation. Thus, equation (12) together with Figure 7 determines the functions $a(\rho)$ and $b(\rho)$.

The first order deviations from axisymmetry in the conservation of mass and angular momentum equations give rise to the following equations for δa_3 and $\delta a_1+\delta a_2$:

$$\delta a_3=-(b/a)(\delta a_1+\delta a_2), \tag{37}$$

$$\frac{d}{d\rho}\left\{\left[\frac{1}{a}+\frac{(\Omega_1-\Lambda_1)}{(\Omega_0-\Lambda_0)}\right](\delta a_1+\delta a_2)\right\}=0. \tag{38}$$

By appropriately choosing initial values of a and b we are free to set $\delta a_3=0$ initially. Equations (37)–(38) guarantee that this condition is maintained. The lowest order nonaxisymmetric contribution to the conservation of quantity $5L/M-C/\pi$ gives an equation for $\delta a_1(\rho)-\delta a_2(\rho)$:

$$\frac{d}{d\rho}\left\{(\Lambda_0+\Omega_0)(\delta a_1-\delta a_2)^2\right\}=0. \tag{39}$$

Since Λ_0 and Ω_0 are known functions of $a(\rho)$ and $b(\rho)$ (by eq. [31]), this equation can be integrated easily to determine the growth of nonaxisymmetry during the collapse.

When the ellipsoid is nearly spherical, these collapse equations simplify considerably, and analytic solutions can be obtained. The radius of the sphere $a(\rho)$ is determined from equation (12) with $a=R$:

$$a(\rho)=(3M/4\pi\rho)^{1/3} \tag{40}$$

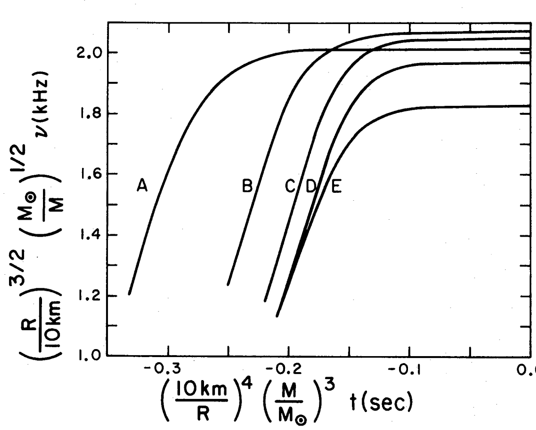

FIG. 7.—The evolution of the asymmetry parameter $\alpha_3(\rho)$ in the collapse of an axisymmetric ellipsoidal model

The analog of equation (36) is vacuous in the spherical limit. The analog of equation (38),

$$\frac{d}{d\rho}(\delta a_1+\delta a_2)=0, \tag{41}$$

implies that the values of δa_3 and $\delta a_1+\delta a_2$ are conserved during the collapse. Finally, the asymmetry of the ellipsoid is determined by the integration of the analog of equation (39) and the use of equation (35):

$$\delta a_1-\delta a_2=(\rho/\rho_0)^{-1/4}[\delta a_1(\rho_0)-\delta a_2(\rho_0)]. \tag{42}$$

c) Gravitational Radiation

After the collapse has been completed, the ellipsoid will evolve toward an axisymmetric state by emitting gravitational radiation. The equations of motion for this process are obtained from the expansions for Λ and Ω in equations (28) and (29) along with the general equation of motion for the lengths of the principal axes, equation (3). These equations simplify to the following form:

$$\frac{d}{dt}(\delta a_1-\delta a_2)=-\frac{32\mathcal{G}\Omega_0^5a^2}{\Lambda_0+\Omega_0}(\delta a_1-\delta a_2), \tag{43}$$

$$\frac{d}{dt}(\delta a_1+\delta a_2)=0. \tag{44}$$

The simple analytic solutions to these equations provide the motivation for considering the nearly axisymmetric case separately:

$$\delta a_1-\delta a_2=[\delta a_1(t_0)-\delta a_2(t_0)]\exp\left[-\frac{32\mathcal{G}\Omega_0^5a^2}{(\Lambda_0+\Omega_0)}(t-t_0)\right] \tag{45}$$

$$\delta a_1+\delta a_2=\text{constant}. \tag{46}$$

Without loss of generality, one can set the constant in equation (46) to zero, by suitably adjusting the values of the constants a and b. Therefore, the general evolution of an almost axisymmetric ellipsoid is given by equation (45) and the conditions $\delta a_3=0$ and $\delta a_1=-\delta a_2$.

The evolution of the asymmetry of the ellipsoid, equation (45), in the spherical limit simplifies to the expression:

$$\delta a_1(t)-\delta a_2(t)=[\delta a_1(t_0)-\delta a_2(t_0)]\exp\left[-\frac{4}{625}\left(\frac{2GM}{ac^2}\right)^3\frac{c}{a}(t-t_0)\right]. \tag{47}$$

As the nearly axisymmetric ellipsoidal figure evolves according to equation (45), gravitational radiation is emitted with a characteristic frequency of $\nu_0=\Omega_0/\pi$ at the luminosity of

$$dE/dt=-\tfrac{64}{5}M\mathcal{G}\Omega_0^6a^2[\delta a_1(t_0)-\delta a_2(t_0)]^2\exp\left[-64\mathcal{G}\Omega_0^5a^2(\Lambda_0+\Omega_0)^{-1}(t-t_0)\right]. \tag{48}$$

The total energy emitted by this system as gravitational radiation (after the time t_0) will be

$$\Delta E_{\rm GR}=\tfrac{1}{5}M\Omega_0(\Omega_0+\Lambda_0)[\delta a_1(t_0)-\delta a_2(t_0)]^2. \tag{49}$$

The spectral density of the exponentially damped sinusoidal waveform has a Lorentzian shape with a line width given by

$$\Delta\nu=32\mathcal{G}\Omega_0^5a^2/\pi(\Lambda_0+\Omega_0) \tag{50}$$

In the nearly spherical limit these equations again simplify considerably. The luminosity is:

$$\frac{dE}{dt}=-\frac{8Mc^3}{5^6a^3}\left(\frac{2GM}{ac^2}\right)^4[\delta a_1(t_0)-\delta a_2(t_0)]^2\exp\left[-\frac{8}{625}\left(\frac{2GM}{ac^2}\right)^3\frac{c}{a}(t-t_0)\right]. \tag{51}$$

The total energy emitted is:

$$\Delta E_{\rm GR}=\frac{Mc^2}{25a^2}\left(\frac{2GM}{ac^2}\right)[\delta a_1(t_0)-\delta a_2(t_0)]^2=0.01\,Mc^2\left(\frac{M}{M_\odot}\right)\left(\frac{10^6\ {\rm cm}}{a}\right)\left(\frac{\delta a_1-\delta a_2}{a}\right)^2, \quad (52)$$

and the gravitational radiation is emitted about the central frequency:

$$\nu_0=\frac{1}{2\pi}\left(\frac{2}{5}\right)^{1/2}\left(\frac{2GM}{ac^2}\right)^{1/2}\frac{c}{a}=1640\left(\frac{M}{M_\odot}\right)^{1/2}\left(\frac{10^6\ {\rm cm}}{a}\right)^{3/2}\ {\rm Hz} \quad (53)$$

with a bandwidth of

$$\Delta\nu=\frac{4}{625\pi}\left(\frac{2GM}{ac^2}\right)^3\frac{c}{a}=1.6\left(\frac{M}{M_\odot}\right)^3\left(\frac{10^6\ {\rm cm}}{a}\right)^4\ {\rm Hz} \quad (54)$$

in this nearly spherical approximation.

IV. DISCUSSION

In the previous sections we have developed the mathematical formalism needed to describe the gravitational collapse and subsequent gravitational radiation to attain axisymmetry within the approximation of the uniform-density ellipsoidal stellar cores. The equations were numerically evaluated for the general nonaxisymmetric ellipsoidal figures considered in § II and analytic solutions were found in the nearly axisymmetric and nearly spherical cases considered in § III. In order to compare the magnitude of the gravitational radiation emitted by the mechanism discussed here with radiation emitted during the dynamic stages of the collapse (see Shapiro 1977, 1979; Saenz and Shapiro 1978, 1979), we consider in detail in this section the radiation from a nearly spherical core with $M=M_\odot$ and $R=10^6$ cm; this model core has an average density of 4.8×10^{14} g cm^{-3}.

The chief step in the use of equations (51) and (52) to estimate the luminosity and total energy radiated is the choice of the asymmetry of the ellipsoid: $(\delta a_1-\delta a_2)/a$. This step is present in all attempts to estimate radiation fluxes. For example, Thorne (1969) uses a fully relativistic analysis of the quadrupole oscillations of realistic neutron star models. With central displacements $\delta r/r=0.1$ he obtains total energies emitted as gravitational radiation in the range $10^{-6}Mc^2\le\Delta E_{\rm GR}\le10^{-4}Mc^2$. If we adopt the same value for the asymmetry of our ellipsoidal models and the same masses and radii, then our total energies from equation (52) are comparable to the upper values in his range.

A more intrinsic way of estimating the value of the asymmetry parameter follows. In the very low angular momentum, nearly spherical case considered here, there is no reason why the rotationally induced asymmetry of the ellipsoid $\delta a_3/a$ should be significantly larger than any other asymmetry, e.g. $(\delta a_1-\delta a_2)/a$. We assume, therefore, that $\delta a_3\approx\delta a_1-\delta a_2$. The value of δa_3, the flattening of the model because of its angular momentum, can be estimated for realistic stellar cores using equation (34). The physical angular velocity of the fluid in the core, Ω_p, is related to the parameters Ω and Λ by $\Omega_p=\Omega-\Lambda$. Young pulsars are formed with angular velocities of the order $\Omega_p=10^3$ s^{-1}; consequently from equation (38) we estimate $\delta a_3/a=10^{-2}$. Using this estimate for $(\delta a_1-\delta a_2)/a$ we arrive at values of $\Delta E_{\rm GR}=10^{-6}Mc^2$ with a maximum luminosity of $(dE/dt)_{\rm max}=2.1\times10^{49}$ ergs s^{-1}. The angular momentum of this model is $L=10^{48}$ g cm^2 s^{-1}. We can compare our estimates with the radiation emitted during the dynamic stages of the collapse as computed by Saenz and Shapiro (1979) for a core with this angular momentum. They find $\Delta E_{\rm GR}\approx10^{-4}Mc^2$ and $(dE/dt)_{\rm max}\approx10^{52}$ ergs s^{-1}. Therefore, the luminosities and total energy emitted will be significantly lower for the effect considered here than in the early dynamic stages of the collapse. The radiation considered here, however, will be considerably more monochromatic than that emitted during an earlier stage of the collapse. A typical value of the spectral density for frequencies near ν_0 is given by: $dE/d\nu\approx\Delta E_{\rm GR}/\Delta\nu=1.1\times10^{48}$ ergs Hz^{-1}. This can be compared to values of $(dE/d\nu)_{\rm max}\approx10^{44}$ ergs Hz^{-1} for comparable models by Saenz and Shapiro (1978). Thus, an appropriately designed gravitational wave antenna may find the radiation from the final approach to axisymmetry easier to observe than the larger burst of radiation from the early dynamic stages of the collapse.

This research was supported in part by National Science Foundation grants to Yale University, the University of California, and Stanford University.

REFERENCES

Chandrasekhar, S. 1969, *Ellipsoidal Figures of Equilibrium* (New Haven: Yale University Press) (E.F.E.).
Boss, A. P. 1980, preprint, NASA Ames.
Detweiler, S., and Lindblom, L. 1977, *Ap. J.*, **213**, 193–199 (Paper I).
Lebovitz, N. R. 1972, *Ap. J.*, **175**, 171–183.
______. 1974, *Ap. J.*, **190**, 121–130.
Lindblom, L., and Detweiler, S. 1979, *Ap. J. (Letters)*, **232**, L101–L105.
Saenz, R. A., and Shapiro, S. L. 1978, *Ap. J.*, **221**, 286.
______. 1979, *Ap. J.*, **229**, 1107–1125.
______. 1980, preprint, Cornell.
Shapiro, S. L. 1977, *Ap. J.*, **214**, 566.
______. 1979, in *Sources of Gravitational Radiation*, ed. L. Smarr (Cambridge: Cambridge University Press).
Thorne, K. S. 1969, *Ap. J.*, **158**, 997.

STEVEN L. DETWEILER: Department of Physics, Yale University, New Haven, CT 06520

LEE LINDBLOM: Department of Physics, Stanford University, Stanford, CA 94305